



Reservoir characterization of the Dokan and Gulneri Formations (Upper Cretaceous) from selected wells in Khabbaz Oil Field, Kirkuk area, Northern Iraq

Fouad M. Qader¹

1Department Geology, College of Science, University of Sulaimani, Sulaimani, Kurdistan Region, Iraq

Email: fuad.qadir@univsul.edu.iq

Article info	Abstract
<p>Original: 22 February 2018 Revised: 30 April 2018 Accepted: 11 June 2018 Published online: 20 June 2018</p> <p>Key Words: Khabbaz Oil Field Reservoir Characterization Dokan & Gulneri Formations</p>	<p>The evaluations of reservoir characterization for Cretaceous Dokan and Gulneri Formations have been selected for this study in Khabbaz Oil Field- Northern Iraq. The Cenomanian Dokan Formation is an open marine oligosteginal limestone ranged in thickness between 21 and 29 meters in this field, and it is overlain by 11 to 14m thick of Gulneri Shale Formation, both are underlying by the thick rock unit of Qamchuqa Formation (Mauddud and Shu'aiba). The full set log data for the seven wells of (Kz-1, Kz-3, Kz-4, Kz-5, Kz-11, Kz-14, and Kz-16) were available, also some general data derived from the wells (Kz-2, Kz-6, Kz-7, Kz-8, Kz-9, Kz-10, Kz-12, Kz-13, Kz-15, and Kz-21). The log data have been used in evaluating the reservoir properties of the two rock units. The detected lithologies from Neutron-Density combination log showed that Dokan Formation is mostly limestone dominated, and the Gulneri Formation is shale rock. From the log data different type of reservoir properties (clay content, porosity, fracture index, and gas crossover) have been estimated. Additional core sample measurements (capillary pressure, porosity, permeability, and thin sections) were used for supplementary analysis.</p>

Introduction

Khabbaz Oil Field is located about 20km NW Kirkuk City in Kirkuk Governorate. The field is surrounded from the northwest by Bai Hassan and Qara Chauq oil fields, from the southeast by Jambour, and Baba Dome of Kirkuk Field located to the east of Khabbaz oil field with about 23km (Fig.1). The first seismic investigation for the area was done by Iraqi Petroleum Company (IPC) in 1955, and they indicated this subsurface structure which is plunges toward northwest (Fig. 2). The first well (Kz-1) at Khabbaz was drilled in August 1976, and the field was brought on stream in March, 1994 by the Northern Oil Company. Production comes from three pay zones: (1) The Tertiary reservoirs;(Middle Miocene Jeribe Formation and Oligocene-Lower Miocene Anah, Azkand, and Azkand/ Ibrahim Formations); (2) Upper Cretaceous reservoirs (Mauddud –Dokan – Kometan Formations); and (3) the Aptian Lower Qamchuqa (Shu'aiba) Formation. The goal of this study is the reservoir characteristic of the Dokan and Gulneri Formations.

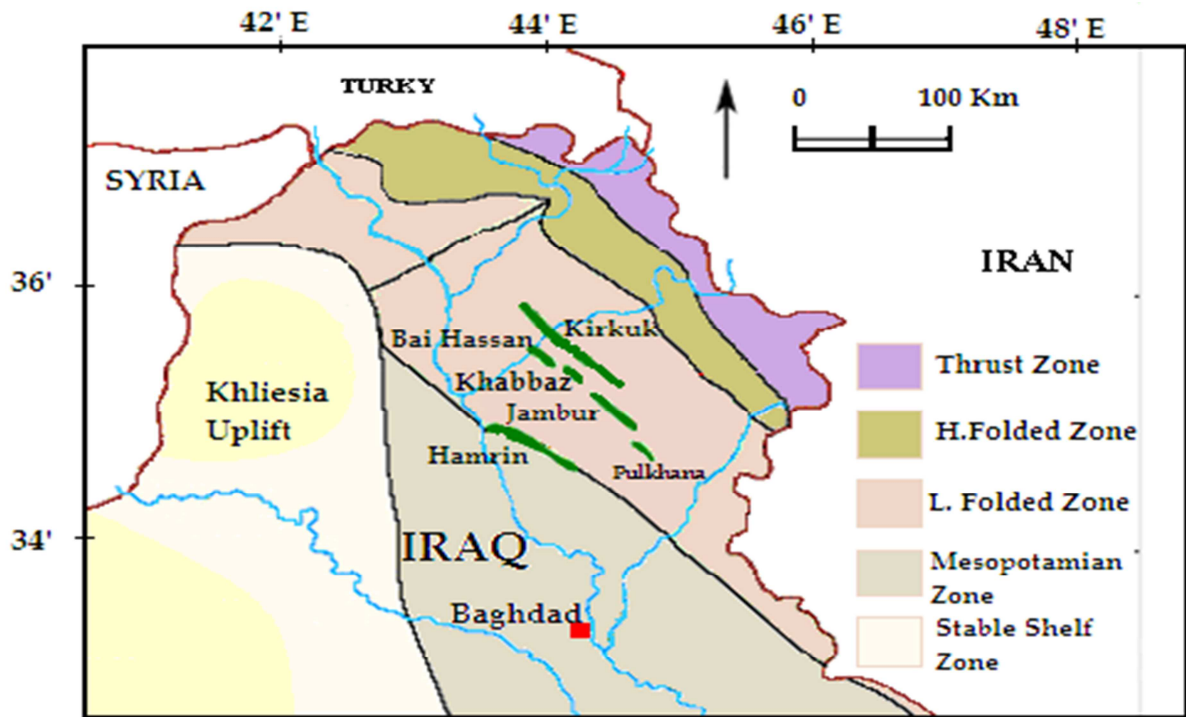


Fig. 1. Regional map of Northern Iraq showing the location of the Khabbaz Oilfield SW of Kirkuk Structure (Qadir, 2008).

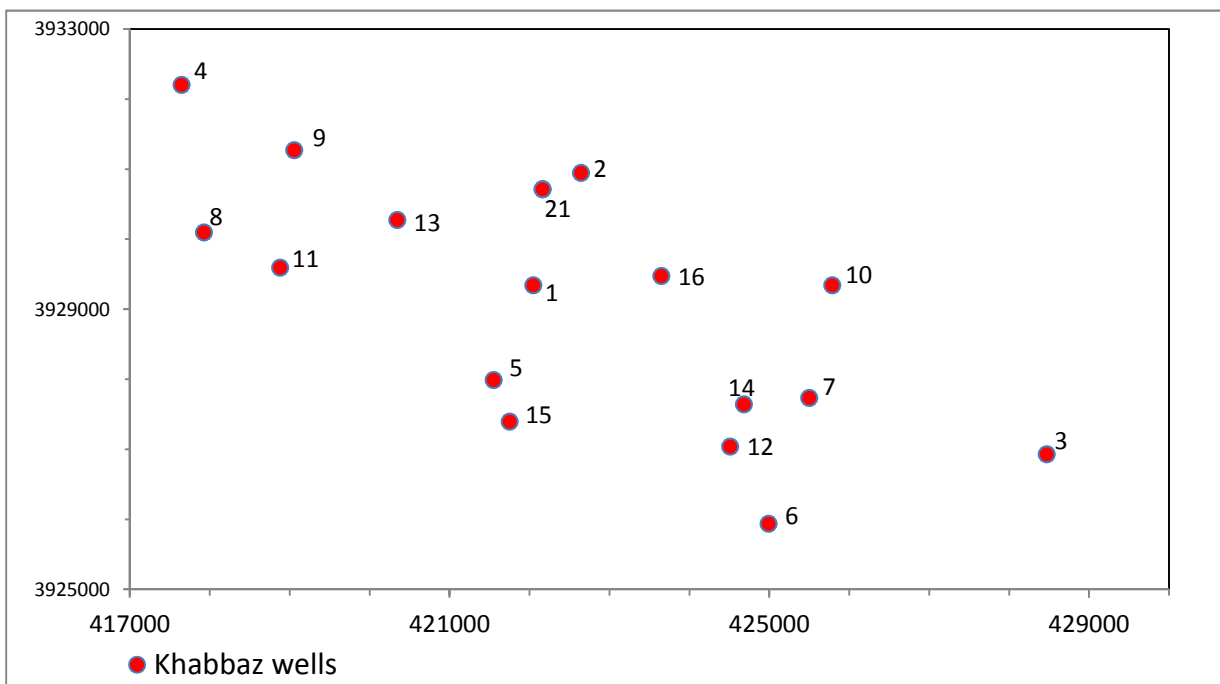


Figure 2: UTM coordinates of the studied wells from Khabbaz Oilfield

Geological Setting

According to the tectonic classification of Iraq (Buday and Jassim, 1987); Khabbaz field located in the Hamrin – Makhul Subzone which is the SW part of the Foot Hill Zone that belongs to the Unstable Shelf. The structure of Khabbaz consists of asymmetrical anticline with northwest-southeast trend (the northeast flank is steeper than the southwest flank). The length of the structure above the top of Mauddud-Dokan Formations is about 13km and its width is approximately 3.5km.

Based on the the final well report of Kz-1, the axis of this small structure runs approximately on the same of Jambour structure and slightly shifts from Bai Hassan structure.

According to the seismic investigation of the area which has done by the Iraqi Petroleum Company in 1955, they indicated a subsurface structure plunging toward northwest, and two major faults intersect the structure to the SE plunge and SW limb (Figs. 3 and 4) and they had a significant influence on reservoir performance.

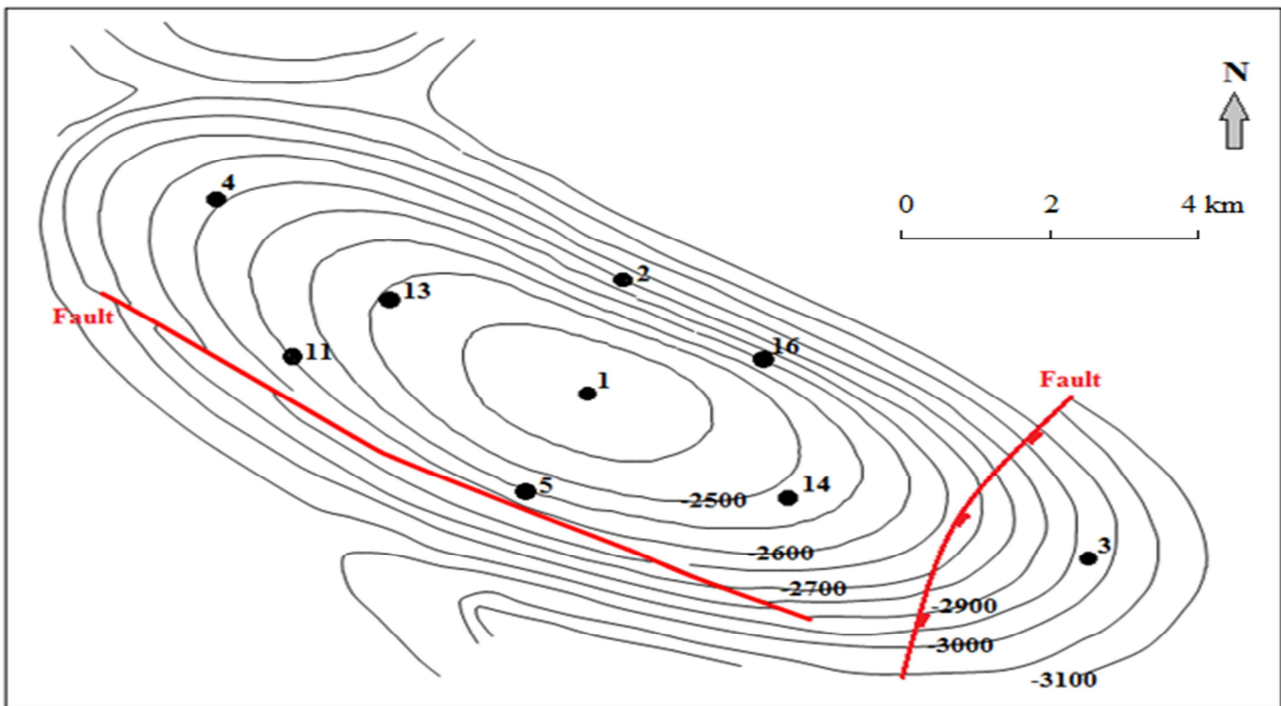


Figure3: Subsea structural contour map of Khabbaz Field on top of the Gulneri-Dokan Formations, (Modified after Iraq Development Potential, 2003)

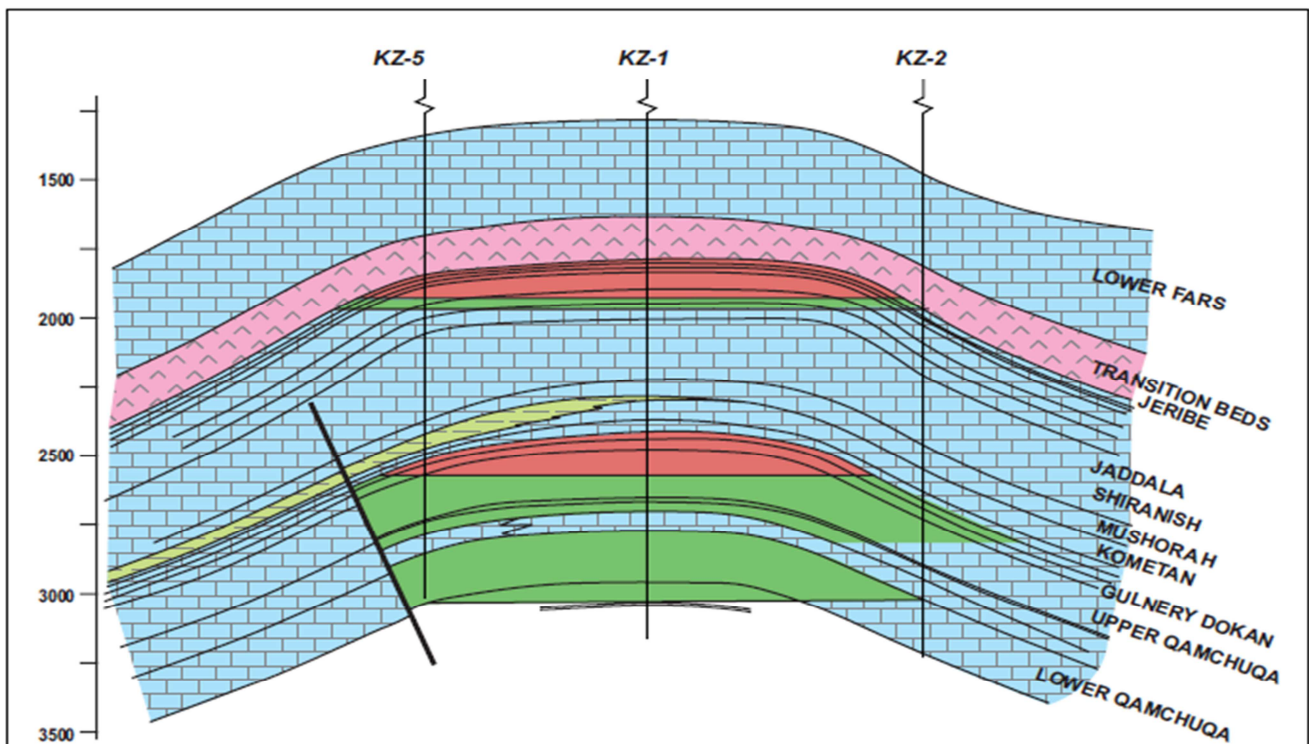


Figure 4: Schematic structural section along the Khabbaz Field showing the major reservoir zones. (Modified after Iraq Development Potential, 2003)

Gulneri Formation

This formation was first recognized and described by Lancaster Jones in 1957 from the site of Dokan Dam in the High Folded Zone, North Northwest of Sulaimanya, where it consists of about 2m of black, bituminous, finely laminated, calcareous, shale with some glauconite and cellophane in the lower part (Bellen et al., 1959). The high bitumen content and dwarfed fossils indicate the formation was deposited in an euxinic environment (Jassim and Buday, 2006). The age of the formation is Lower Turonian as recorded by Bellen et al. (1959). The formation is separated by unconformities of both the underlying Dokan and the overlying Kometan Formations (Buday, 1980). According to the final geological well reports in the subsurface sections (Kz-1, Kz-2, Kz-11, and Kz-14) the lithology in the studied area are composed of lamination, black to dark grey shale,

bituminous, rare pyrite and glauconite spots in the fossil casts. The thickness ranges between 11 and 14m along the Khabbaz field.

Dokan Formation

The Dokan Limestone was formerly included in the Kometan Formation (Jassim and Buday, 2006). It was first described by Lancaster Jones in 1957 (Bellen et. al., 1959). The type locality is on the site of Dokan Dam in the High Folded Zone North Northwestern of Sulaimaniya Northeastern Iraq. It is composed of four meters light colored grey and; white- weathering oligosteginal limestones, locally rubbly, with glauconitic coatings of constituents pebble-like masses (Bellen et. al.,1959). However in the subsurface sections, the color of the limestone is mostly dark grey, shaly or marly (Buday, 1980). The distribution of the formation is relatively restricted. The main area of its distribution and of its outcrops too, is the High Folded and Foothill Zones, roughly to the Southeast of Mosul uplift (Buday, 1980).

According to the final geological well reports (Kz-1, Kz-2, Kz-11, Kz-14); this formation is comprised of brown to grey limestone, typically Oligosteginal dense limestone, tight locally micro fractured, with stylolites, glauconite spots in the upper contact, rare detrital limestone streaks were recorded, with Oligostegina, Globogerine Fauna sp. and other shell fragments. The thickness ranges between 21 and 29m all over the Khabbaz field. The formation is overlain by Gulneri Formation and underlain by Mauddud (Upper Qamchuqa) Formation (Figure 5).

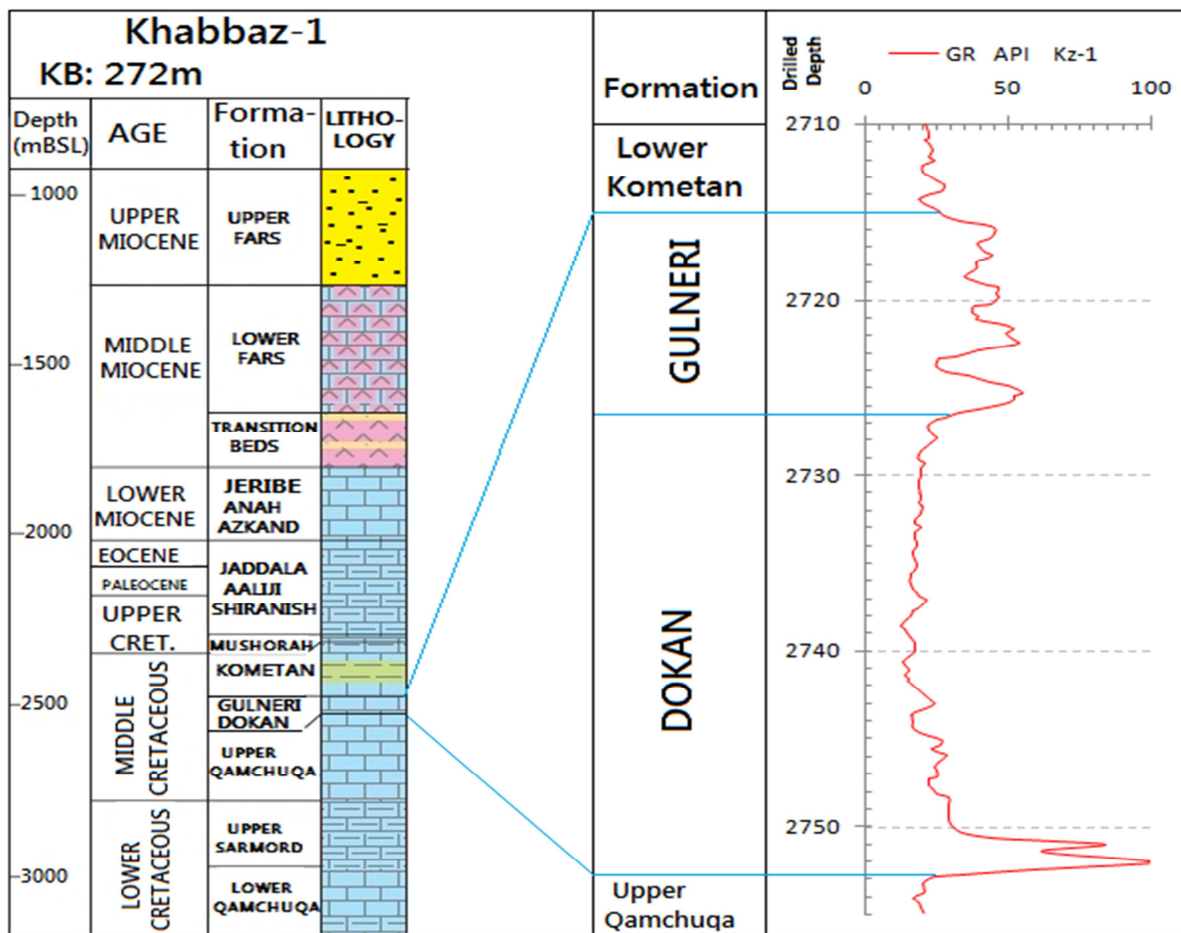


Figure 5: General stratigraphic column showing the lithologies, GR log characters, and nomenclature of the Gulneri-Dokan Formations in well Kz-1.

Materials and Methodology

The main tools that are used in this study are different types of logs, namely: Neutron Log (CNL type), Density Log (FDC type), Sonic Log (BHC type), Gamma Ray (GR), and Caliper Log; from the wells Kz-1, Kz-3, Kz-4, Kz-5, Kz-11, Kz-14 and Kz-16. Since the log was as old sheet graph; first the graph was converted into

digit data using the graph digitizer software (getdata222) and later the digitized data reprocessed and plotted by excel software.

The available core tests included porosity, permeability, and Pore Size Distribution by Mercury injection, in addition to the thin sections.

Rock properties obtained from NOC final well reports were used in calibrating the outputs of the log analysis. Table 1 shows the depth intervals and thicknesses of the studied formations in the eleven wells of Khabbaz oil field.

Table-1: Depth interval and thickness of the Gulneri and Dokan Formations in the wells. (Depth measured from RTKB Datum)

Wells	Formations	Depth interval (m)	Thickness (m)
Kz-1	Gulneri	2715-2727	12
	Dokan	2727-2753	26
Kz-2	Gulneri	2991-3003	14
	Dokan	3003-3025.5	22.5
Kz-3	Gulneri	3169.5-3181	11.5
	Dokan	3181-3203	22
Kz-4	Gulneri	2938.5-2950	11.5
	Dokan	2950-2979	29
Kz-5	Gulneri	2796.5-2808	11.5
	Dokan	2808-2832.5	24.5
Kz-7	Gulneri	2893-2904	11
	Dokan	2904-2931	27
Kz-11	Gulneri	2848-2859	11
	Dokan	2859-2886	27
Kz-12	Gulneri	2901-2912	11
	Dokan	2912-2933.5	21.5
Kz-13	Gulneri	2767-2778	11
	Dokan	2778-2805.5	27.5
Kz-14	Gulneri	2779-2790.5	11.5
	Dokan	2790.5-2811.5	21
Kz-16	Gulneri	2870.5-2882	11.5
	Dokan	2882-2906	24

Well Correlation

Two cross sections were drawn across the field based on the GR log responses; one of the sections was selected through the wells Kz-4, Kz-1, Kz-14, and Kz-3 the longitudinal profile along the field; from northwest plunge to the southeast plunge as shown in Figure 6. The section shows a normal fault cutting the SE plunge of the field between wells Kz-14 and Kz-3, from that section it is clear that thickness of Gulneri Formation is almost constant along the field with ranges between 11 to 12m, while the Dokan Formation has maximum thickness in well Kz-4 in the NW plunge of the structure, which reaches 29m and it decreases toward NE direction from 26m in Kz-1 to 21m in the Kz-3 the SE end of the field.

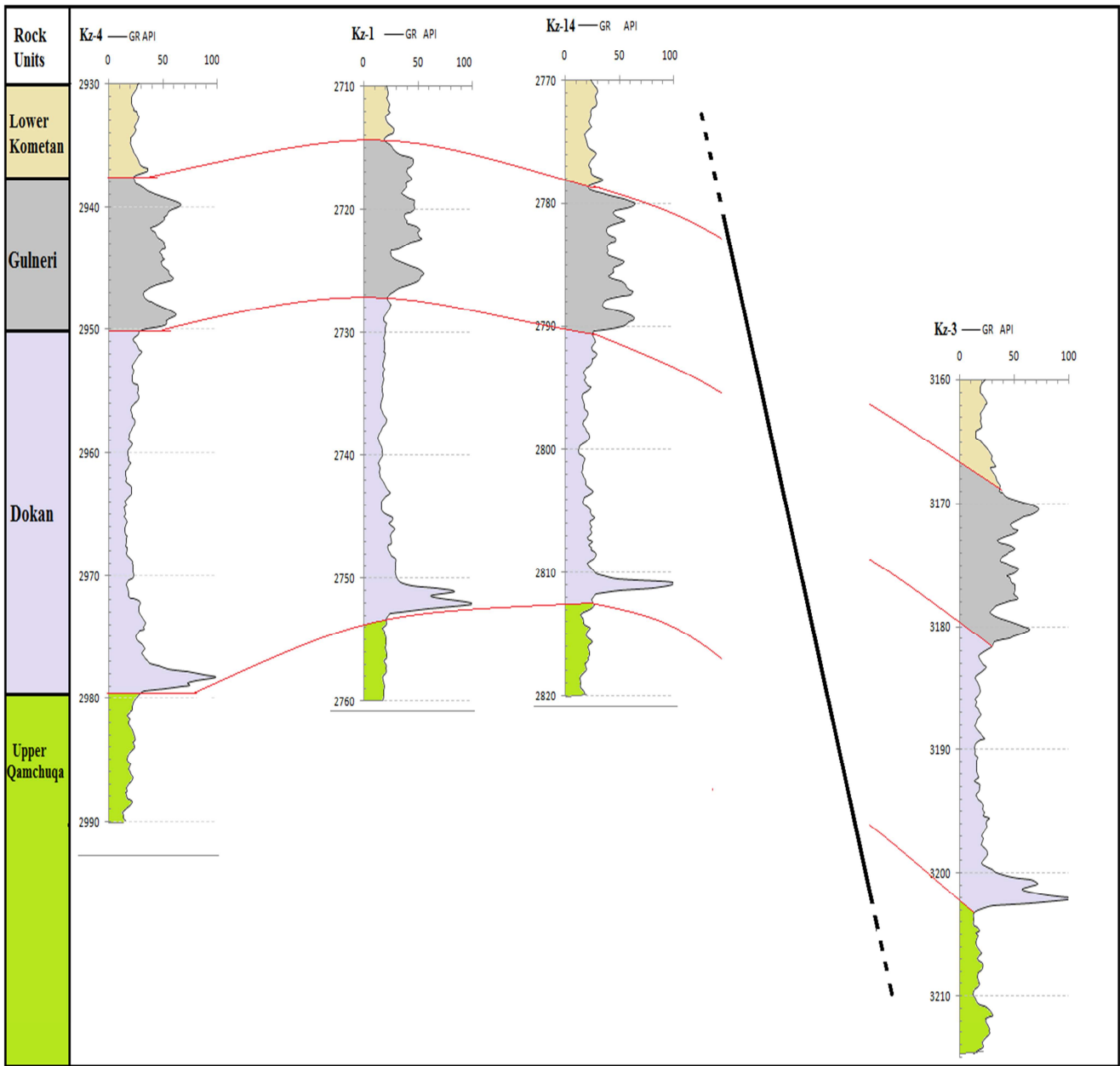


Figure 6: Structural cross section and well correlation from NW plunge to the SE plunge of the Khabbaz field. (Depth measured from RTKB Datum).

The second GR log correlation section was made along transverse path from well Kz-11 at the SW limb to the Kz-16 in the NE limb passing along the Kz-1 in the crest of the structure (Figure 7). From that figure it is clear that there is no significant change in the thickness of Gulneri Formation, which also ranges from 11 to 12m along this section. The thickness of the Dokan Formation increases toward the SW limb which is started with 24m in Kz-16 in the NE limb, to 26m in the Kz-1 in the crest of the structure and 26.5m in the Kz-11 at the SW limb.

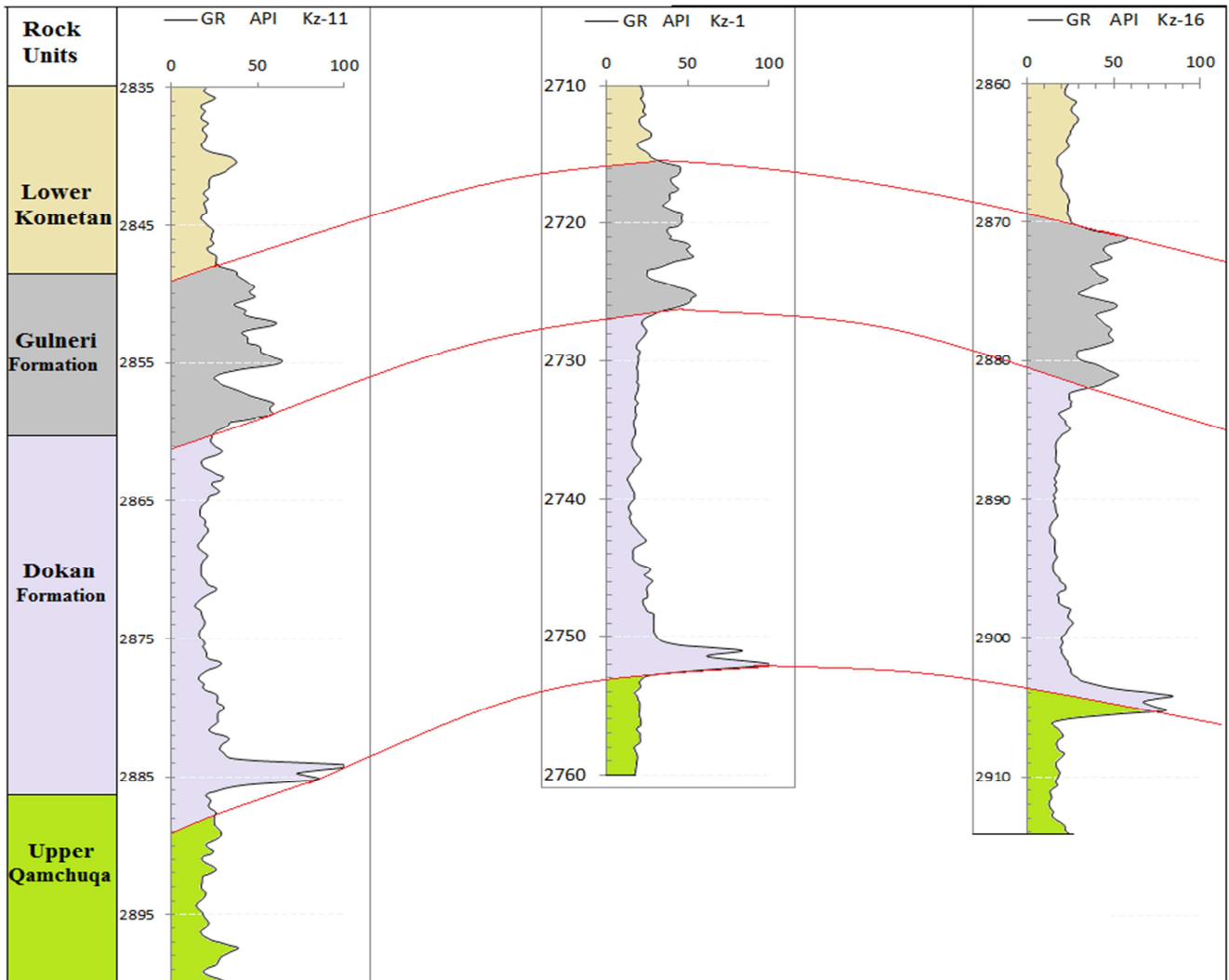


Figure 7: Well correlation along the section from SW limb to the NE limb of the Khabbaz field. (Depth measured from RTKB Datum).

Shale Volume Calculation

Since shale is usually rich of the radioactive elements more than sandstone or carbonates, gamma ray log is a good tool to calculate volume of shale in reservoirs. The volume of shale can then be applied for analysis of shaly formation (Asquith and Gibson, 1982). If one considers the maximum average gamma ray log value to be 100% pure shale, and the lowest value to indicate shale free; the gamma ray log will give the volume of shale from simple calculation (Rider & Kennedy, 2011):

$$\text{Volume of Shale (V}_{sh}\%) = \frac{GR \log - GR \min}{GR \max - GR \min}$$

Where:

- GRlog = Gamma Ray Reading of Formation
- GRmin = Minimum Gamma Ray (clean sand or carbonate)
- GRmax = Maximum Gamma Ray (shale)

According to Ghorab (2008) reservoir rocks classified on the basis of percentage of shale or shale volume (V_{sh}) into :Clean zone (V_{sh}<10 %), Shaly zone (V_{sh}10 – 35%), and Shale zone(V_{sh}> 35 %). After applying this classification, it appears that the majority of the Gulneri Formation section in all wells can be classified as very high shaly to shale zone. Regarding the Dokan Formation the majority of the section represent the clean zone with the exception of two thin intervals at the most upper part and most lower part which they exceed the 10% shale volume and classified as shaly zones. Based on this result the Gulneri Formation considered as non-reservoir unit and it is excluded from further evaluation; and the detail evaluation will focused on the Dokan Formation.

Lithology Determination from Porosity Logs

When these logs are used individually, each of them has a response to lithology which must be accounted for. But when used in concert, two or three at a time, lithology can be estimated and more accurate porosity derived, and much useful information can be gathered by combining the measurements of more than one porosity tool (Bateman, 1985).

The neutron-density crossplot (combination) is used to illustrate and differentiate the common reservoir lithologies (sandstone, limestone, and dolomite), shale and some evaporites (Schlumberger, 1988). According to Rider (2002) both the density and neutron logs are difficult to use for lithology recognition separately, but if they are combined, they become probably the best available indicator.

The measurements of the two logs for the studied formation in the seven wells of Kz-1, Kz-3, Kz-4, Kz-5, Kz-11, Kz-14, and Kz-16 are used to recognize the lithologies using the Neutron-Density crossplot proposed by Schlumberger (1988) for the case of fresh water based drilling mud.

Figures 8 and 9 show the lithology of Dokan Formation in the selected wells. The lithology of Dokan Formation shows dominance of limestone, where the points well matched with the Limestone line, with some shifting to the dolomitic limestone or toward argillaceous limestone zone under the effect of gas. The scattered points belong to the uppermost and lowermost shaly parts of the formation.

The average porosity from the cross plot in wells Kz-1 and Kz-4 ranged between 5 and 15%, and in wells Kz-5, Kz-11, and Kz-16 the porosity ranged from 3 to 10%. Whereas the porosity decreased toward the southeast plunge of the field in wells Kz-14 and Kz-3 especially in the latter one to be nearly of zero porosity.

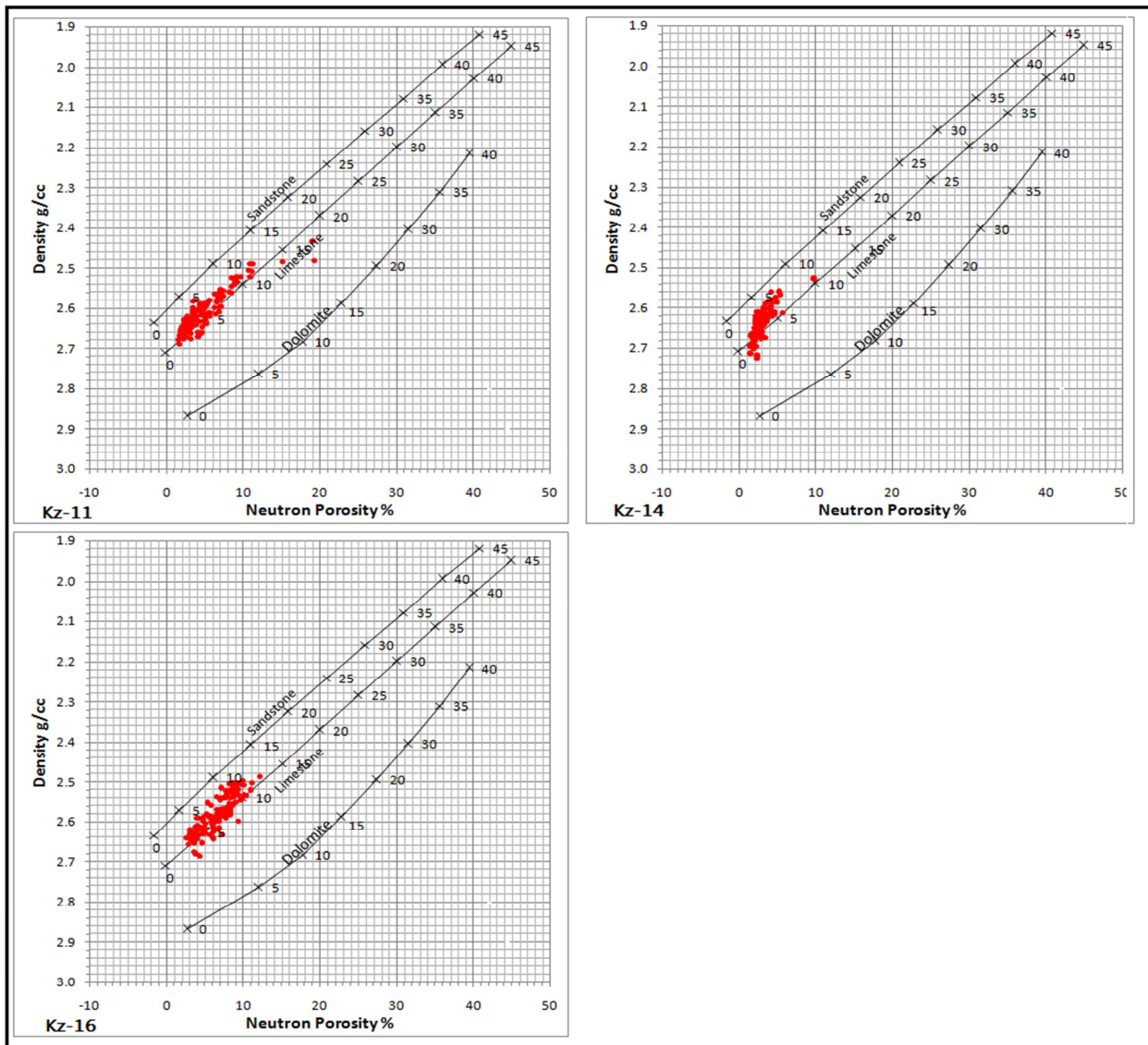


Figure 8: N-D cross plot for lithology identification of the studied formations in the wells Kz-1, Kz-3, Kz-4, and Kz-5.

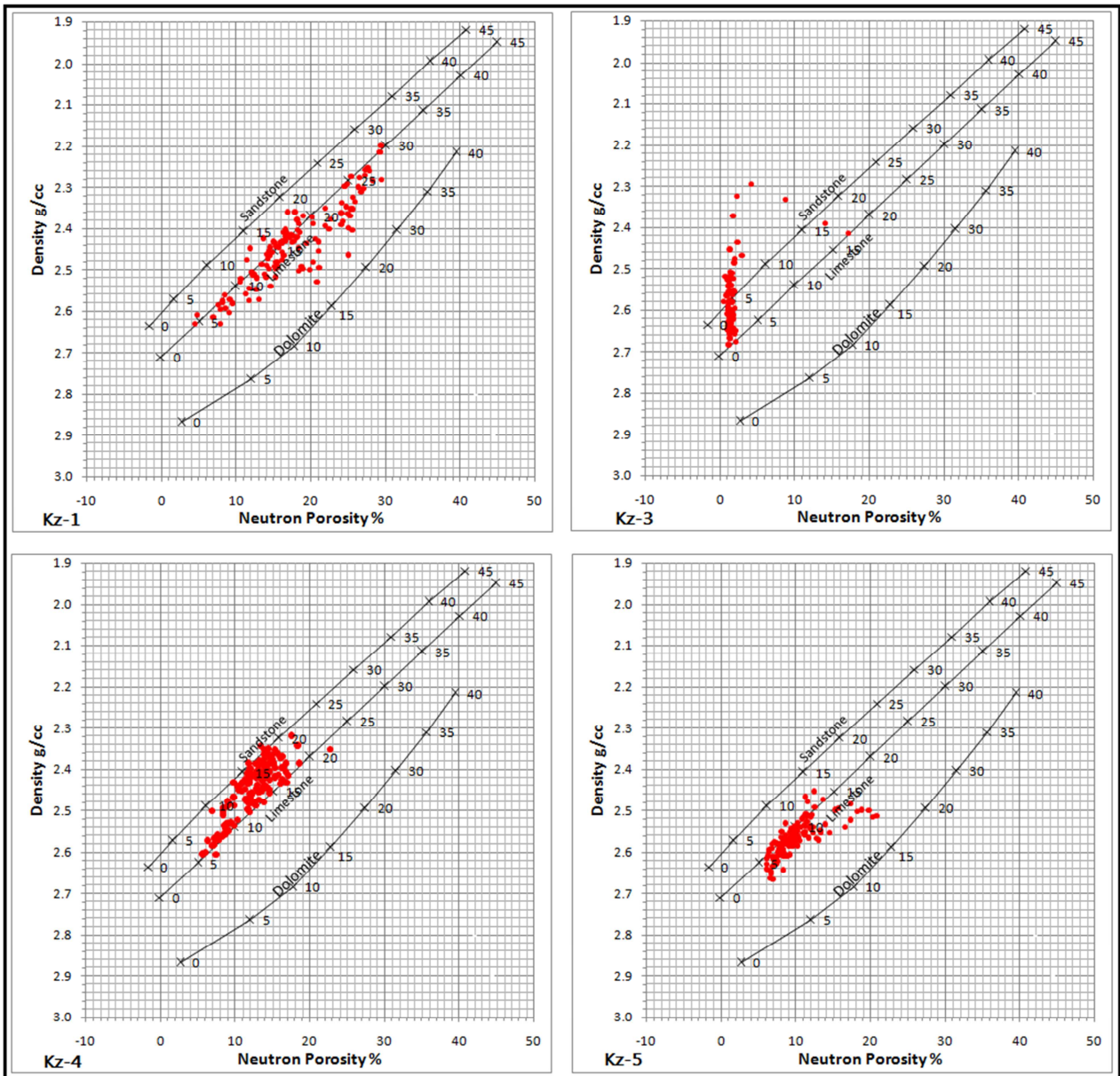


Figure 9: N-D cross plot for lithology identification of the studied formations in the wells Kz-11, Kz-14, and Kz-16.

Porosity measurement

The porosity raw data were measured from three porosity logs (sonic, density, and neutron) using “getdata222.exe” program; with five digitized points per meter from each log. After processing and plotting of these porosity values against the lithology column led to the prediction that the Dokan Formation is represents one reservoir unit. Due to low shaleness of Dokan Formation, the direct measured log porosities were used without shale corrections.

The porosity was calculated from three common types of porosity logs including Neutron, Density, and Sonic logs, the followings are short description of each one:

Neutron Log... The tool consists of a fast neutron source and two detectors, both source and detectors are pressed against the borehole wall, and it is measured liquid (water or oil) filled porosity; the neutron curve displayed in porosity unit and referenced to a specific lithology. In the Dokan reservoir, the standard limestone lithology was considered.

Density Log...The Density log is measured in gram per cubic centimeter, g/cm^3 , and is indicated by Greek letter ρ (rho). The bulk density (ρ_b) is the density of the entire formation as measured by the logging tool. The formula for calculating density porosity is:

$$\Phi_D = \frac{pma - pb}{pma - pfl}$$

Where:

Φ_D = density derived porosity

pma = matrix density (in this study used standard limestone 2.71 g/cm³)

pb = formation bulk density (the log reading)

pfl = fluid density (fresh drilling mud; 1.0 g/cm³ used for this study)

Sonic Log...The sonic tool measures the interval transit time, Δt , or the time in microseconds for an acoustic compressional wave to travel through one foot or meter of formation, along a path parallel to the borehole (reciprocal of velocity). $\mu\text{s}/\text{ft}$ or $\mu\text{s}/\text{m}$. The interval transit time (Δt) is related to porosity; with increasing the Φ , Δt also increases (if other things are constant).

The borehole-compensated (BHC) devices were used in Khabbaz oil field and the Wyllie time-average equation (Asquith and Krygowski, 2004), was utilized:

$$\Phi_S = \frac{\Delta t \log - \Delta tma}{\Delta tfl - \Delta tma}$$

Where:

Φ_S = Sonic derived porosity.

Δtma = interval transit time in the matrix (Δt limestone is used)

$\Delta tlog$ = interval transit time in the formation (measured by log)

Δtfl = interval transit time in the fluid in the formation (freshwater mud = 189 $\mu\text{sec}/\text{ft}$; used in this study)

Neutron-Density combination porosity: the combination of the both neutron and density tool measurements is the very common used for the estimation of the average porosity (Φ_{N-D}), this gives a more accurate porosity (Selley, 1998; Asquith and Krygowski, 2004), and the following formula was used:

$$\Phi_{N-D} = \frac{\Phi_N + \Phi_D}{2}$$

Fracture analysis

The fractures have the great role to improve the reservoir properties (Porosity and permeability) especially in carbonate rocks, so the important portion of the world's hydrocarbon reserves belongs to the fractured carbonate reservoir, and the description of the fracture system is the essential petrophysical evaluation of the reservoir.

Sonic log measure the uniform inter-particle or inter-crystalline porosity (primary porosity), while the average measured porosity by Neutron-Density log is considered as total porosity. When the sonic porosity (Φ_S) are compared with the total neutron and density porosity (Φ_{N-D}); the different between them is the secondary porosity (fractures, cavities, vugs .. etc).

$$\Phi_f = \Phi_{N-D} - \Phi_S$$

Where:

Φ_f = fracture porosity (secondary porosity).

Φ_{N-D} = neutron-density porosity (total porosity).

Φ_S = sonic porosity (primary porosity).

The calculated total porosities from neutron-density logs (Φ_{N-D}) and primary porosities from sonic log (Φ_S), in addition to fracture porosity (secondary porosities) for the Dokan Formation revealed a noticeable different porosity, with different fracturing intensities in the different wells. The porosity ranged between 0.036 and 0.144. According to North (1985)'s classification of porosity; the Dokan reservoir in this field considers as of negligible to fair porosity reservoir.

The Dokan reservoir shows the highest porosity in the wells Kz-1 and Kz-4, with reasonable intensities of fracturing, and the lowest porosity belongs to the Kz-14. Despite the low porosity in Kz-3, the majority of the porosity is related to fracturing which comprises 65% of the total porosity; this is related to the location of the well on the hanging wall of the normal fault in the SE plunge of the structure (Fig.3)

Figures 10, 11, 12, and Table 2, summarize the different porosities and fracturing in seven wells distributed all over the Khabbaz field.

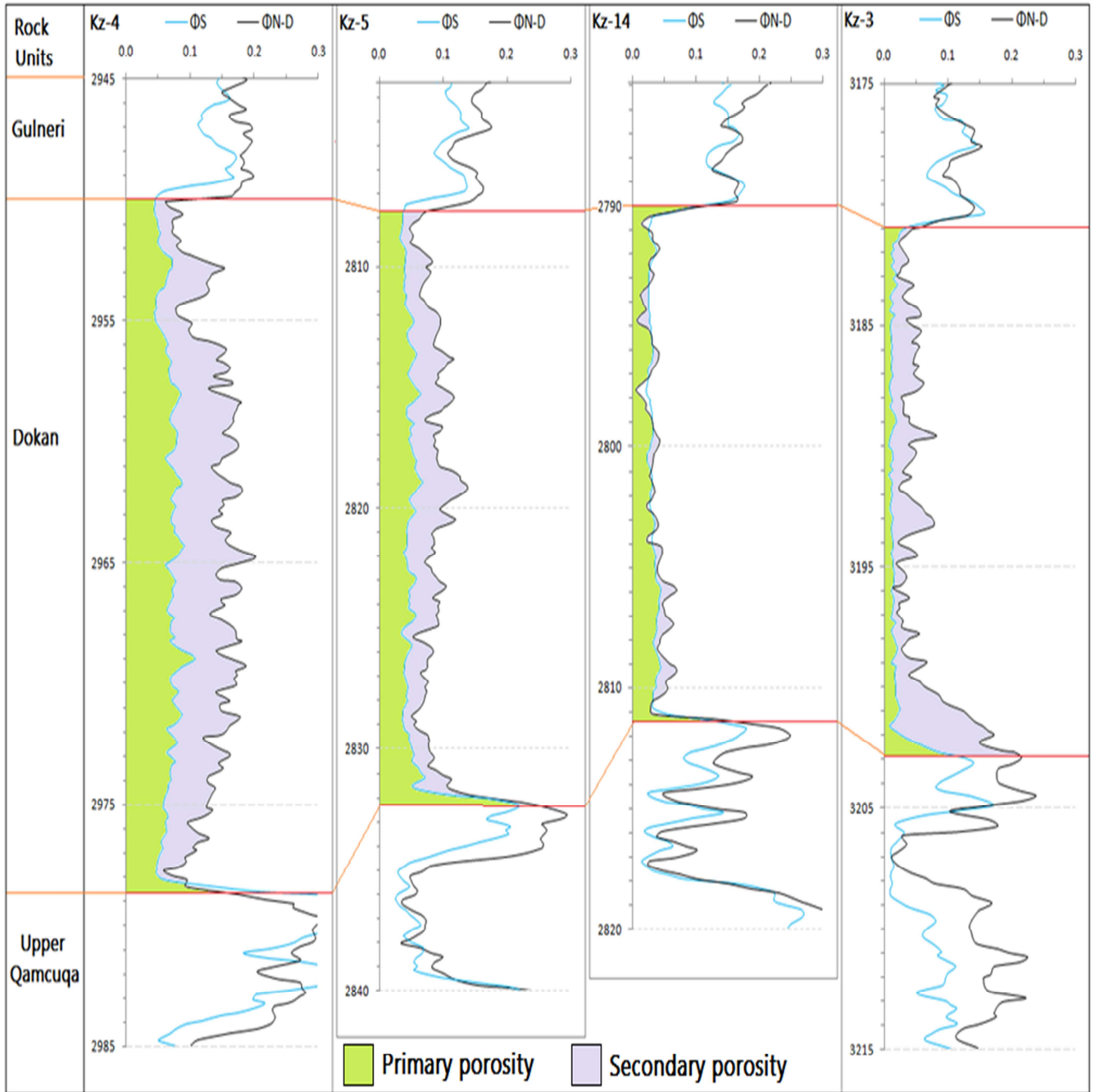


Figure- 10: Primary and secondary (fracture) porosity plot for the Dokan Formation in the studied wells of Kz-4, Kz-5, Kz-14 and Kz-3.

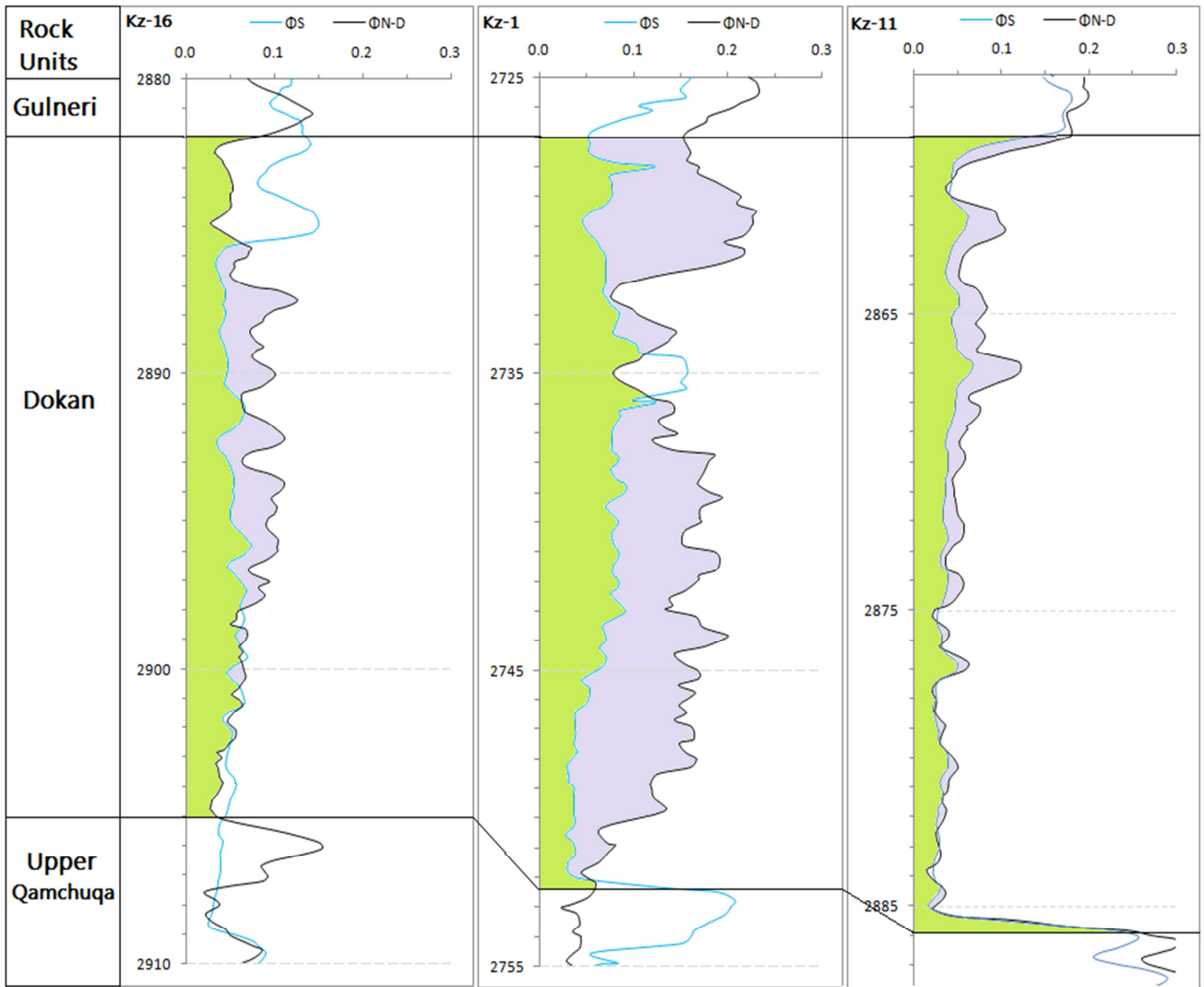


Figure- 11: Primary and secondary (fracture) porosity plot for the Dokan Formation in the studied wells of Kz-16, Kz-1, and Kz-11. (Depth measured from RTKB Datum).

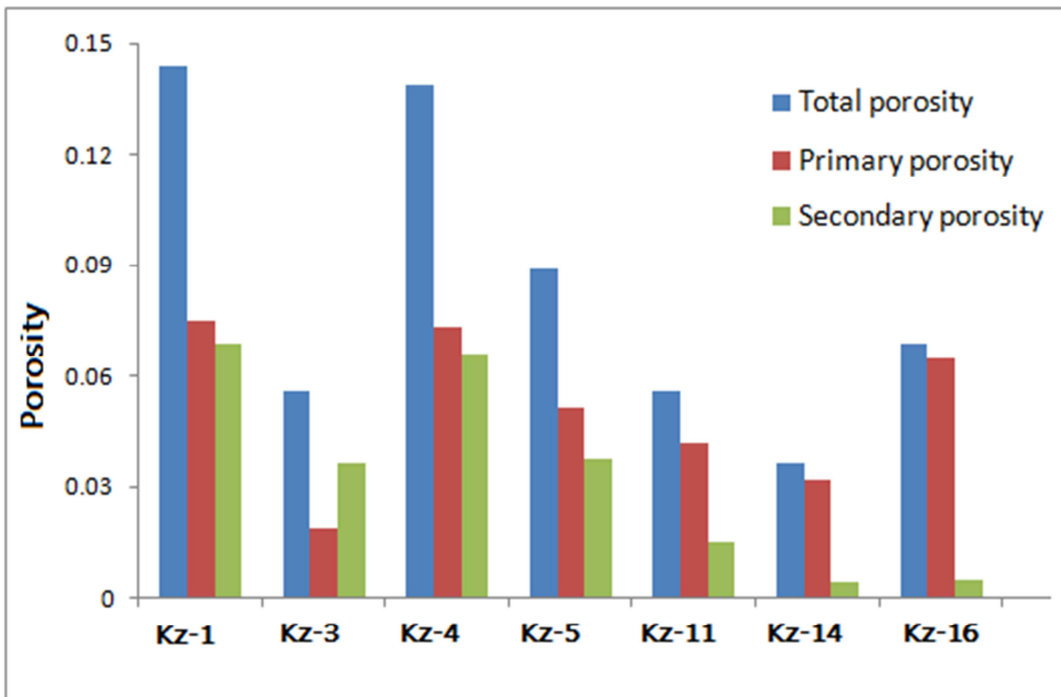


Figure- 12: Total, primary, and secondary (fracture) porosity histogram for the Dokan Formation in all studied wells.

Table- 2: The summary of the total porosity, primary and secondary porosities with their ratio.

Wells	Total Porosity	Primary porosity	Secondary Porosity	Primary Porosity ratio	Secondary porosity ratio
Kz-1	0.144	0.075	0.069	0.519	0.481
Kz-3	0.056	0.019	0.036	0.347	0.653
Kz-4	0.139	0.073	0.066	0.523	0.476
Kz-5	0.089	0.0516	0.0375	0.579	0.421
Kz-11	0.056	0.042	0.015	0.741	0.259
Kz-14	0.036	0.032	0.004	0.897	0.103
Kz-16	0.069	0.065	0.005	0.933	0.067

Neutron –Density Crossover

Another technique using the neutron and density logs and the identification of the curve patterns is that of gas identification. Gas in the pores causes the density porosity to be too high (gas has lower density than oil and water) and causes the neutron porosity to be too low (due to lower concentration of hydrogen atoms in gas than in oil or water). In gas zone, the neutron porosity is less than the density porosity, and the two porosity curves cross over each other and this is called crossover (Asquith and Krygowski, 2004).

Figure 13 shows the two porosity curves for Dokan section; neutron porosities (red curve) (Φ_N) and density porosities (black curve) (Φ_D). The crossover of these two curves is observed clearly along all sections with different intensities, this result was expected as Dokan Formation is underlain by a thick oil column of Mauddud (U. Qamchuqa) and Shu'aiba (L. Qamchuqa) reservoirs (Qader, 2008 and Qader and Al-Qayim, 2016) and it is hosting a thick gas cap. The crossover is clearer in the wells Kz-3 and Kz-4 the two ends of the field; this may be due to impregnated the fractures and large porous by heavy oil near the crest of the structure more than margins during the earlier oil accumulations, before it displacements by cap gas.

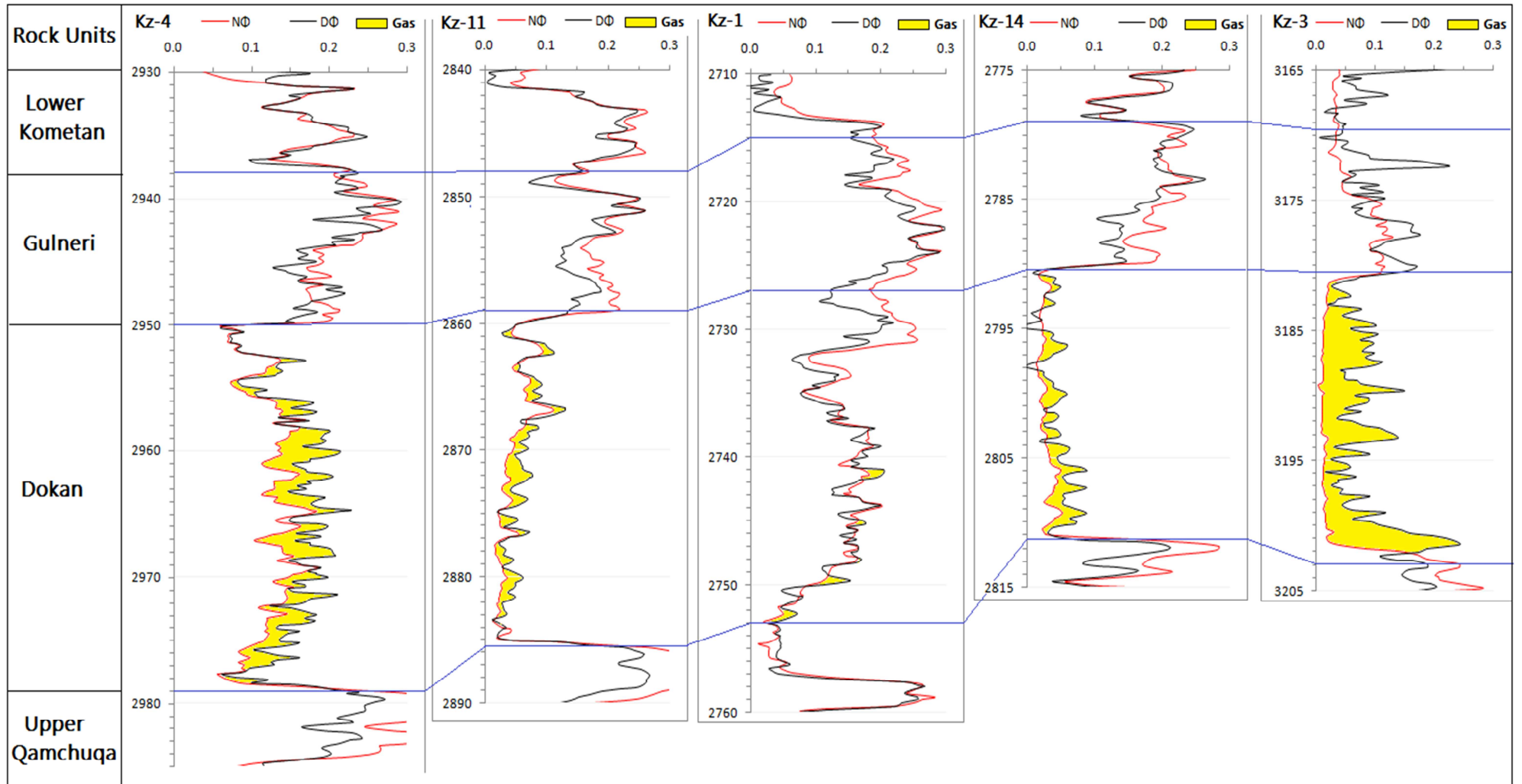


Figure-13: Crossover (Gas effect) of Neutron and Density porosity curves as appeared in the studied well sections. (Depth measured from RTKB Datum).

Core sample measurements

Core samples from well Kz-2 were examined from the intervals between 3004.1 and 3025.3; measured data were supplied by the North Oil Company (NOC). The test included porosity, permeability, and Pore Size Distribution by Mercury Injection, in addition to the thin sections.

The porosity and permeability of core plugs were determined by measuring the grain volume using the air expansion method using a Kirkuk-modified Washburn & Bunting porosimeter, and measuring the bulk volume by the buoyancy method using mercury.

Porosity: porosity of small plugs (1x1 inch) was determined by measuring the grain volume by the air expansion method and bulk volume by the buoyancy method using mercury, the average porosity for 52 plugs was 5.9%.

The porosity of the large plugs (1 1/2 inch) was determined by the brine saturation method. The plugs were weighted dry in air and then saturated with brine and the weight of the saturated plug was determined under brine and in air. 12 plugs gave an average porosity of 8.7%, which is higher than the corresponding porosity of the small plugs.

Permeability: Due to fracturing of the samples most of the measurements were failed; and permeability test were carried out on 38 small plugs (1x1 inch) using Rushka method gave an average of 0.95md; most of the plugs had zero permeability. Also Slip-Corrected gas permeability is used for measuring flow rates at series of pressure, and by applying Darcy Law permeability was determined. Most of the large plugs were fractured and could not be used in this test; only 2 plugs gave result of 0.27 md.

Thin sections: from testing of the few available thin section samples it appears that the microfacies is composed of mainly matrix rich wackestone - partial packstone with presence of planktonic foraminifera from deep marine environment (Figure 14).

From reservoir prospective, the primary porosity is mainly composed of matrix porosity (microporosity). Secondary porosity comes from fractures which are some of them filled by secondary calcite (see figure 14-a, and b on the left sides). Pressure solution is present indicating burial environment (see photo figure 14-a on the right side). Very poor permeability is expected.

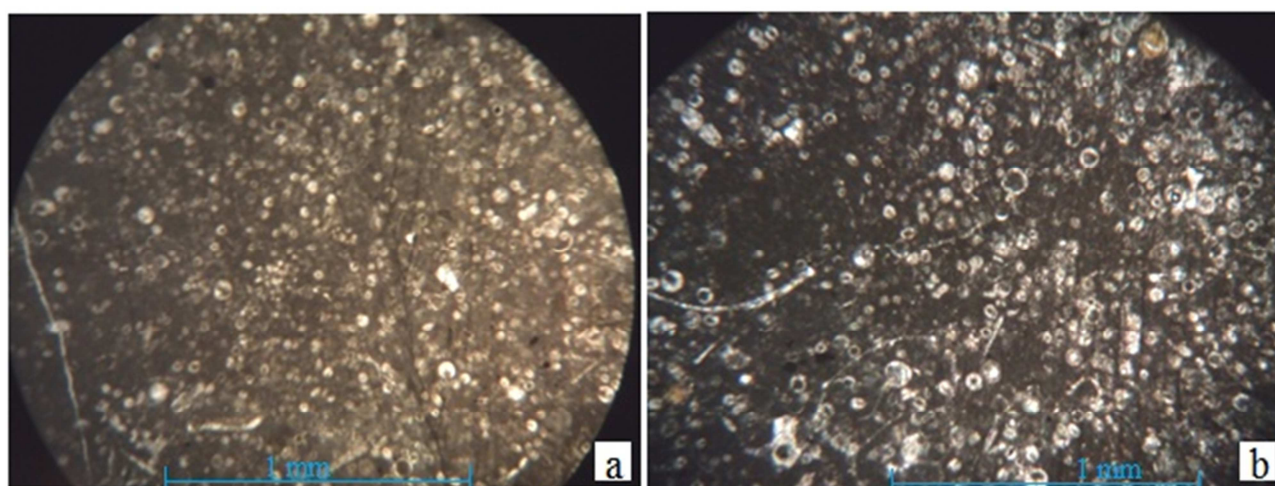


Figure-14: Oligosteginal foraminiferal wackestone- partial packstone

Mercury Injection Experiments: During this drainage process, the pressure is increasing to pass the required pressure to form a continuous layer of the non-wetting phase (Mercury) through the pore spaces, a small plug in depth 3016.8m at Kz-2 was selected in this test and mercury (the non-wetting phase) was injected into the pores of the plug at stages of pressure up to 5014 psi, and the corresponding percentage mercury saturation is calculated, as given in the Table-3

Table 3: Pore Size Distribution by Mercury Injection

Pressure (psi)	Equivalent Pore Radius (Micron)	% Pore Space Hg Saturation
8.1	11.1	3.06
13	6.92	5.13
17.8	5.06	5.88
22.6	3.98	7.56
27.5	3.27	7.81
33.2	2.71	7.94
39	2.31	8.13
46.2	1.95	8.19
114.1	0.789	15.94
214.1	0.42	30.31
314.1	0.287	38.94
464.1	0.194	47.25
764.1	0.118	57.31
1014.1	0.089	63
1514.1	0.059	68.94
2014.1	0.045	75
3014.1	0.03	76
4014.1	0.022	80.56
5014.1	0.018	81.75

The capillary pressure is building up before Mercury (the non-wetting phase) displaces the wetting phase beyond the threshold pressure Figure-15. The threshold pressure point has been experimentally proven by monitoring electrical resistance across a sample and noting the pressures at which continuity occurs (Katz and Thompson 1986, 1987). The invasion saturation of Mercury is increasing depending on the pore-throat size. This increase will be rapid above threshold point and has been successfully utilized Dewhurst et al., 2002. Remarkable increase has been observed in mercury saturation for pore size of less than 2-micron Figure-16. According to Figure-16, threshold pressure can be reached at mercury saturation of about 8-9 %. Hence, the displacement of wetting phase by mercury at which continuous non-wetting phase will be formed will take place at pores of less than 2-microns. This is obviously clear in Figure-17, where the capillary pressure curvature starts at pores within less than of 2-microns.

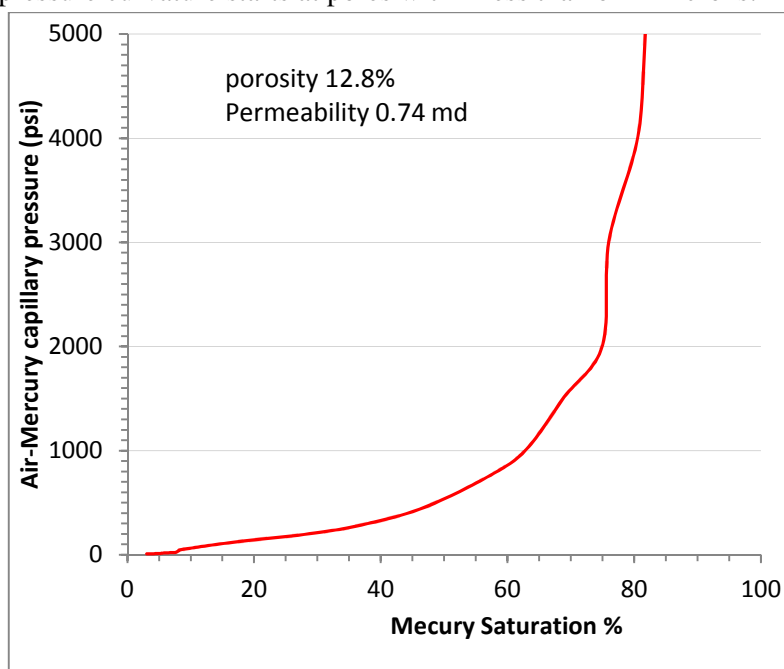


Figure 15: Mercury Capillary Pressure vs Mercury Saturation

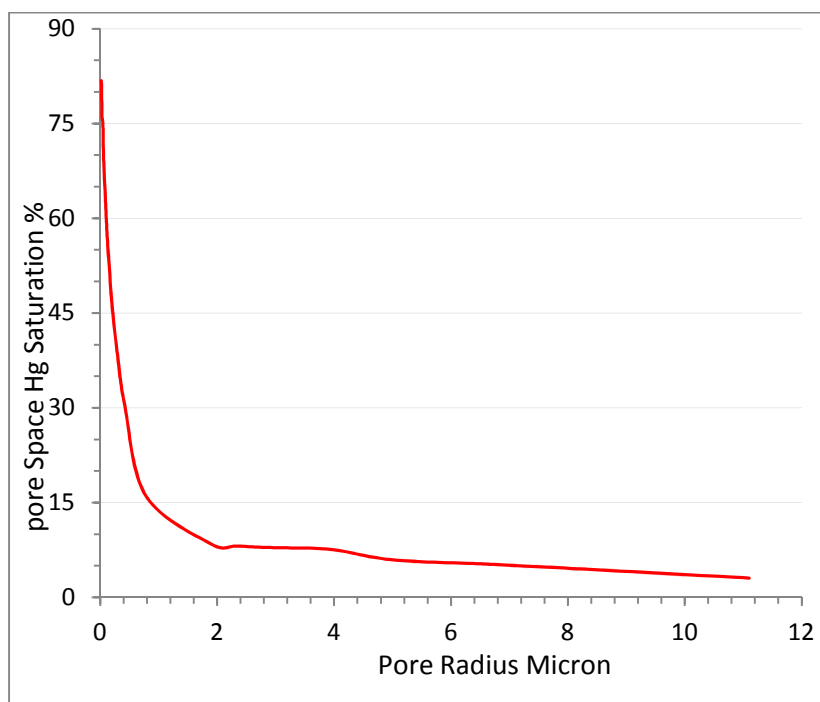


Figure-16: Mercury Saturation vs Pore Radius

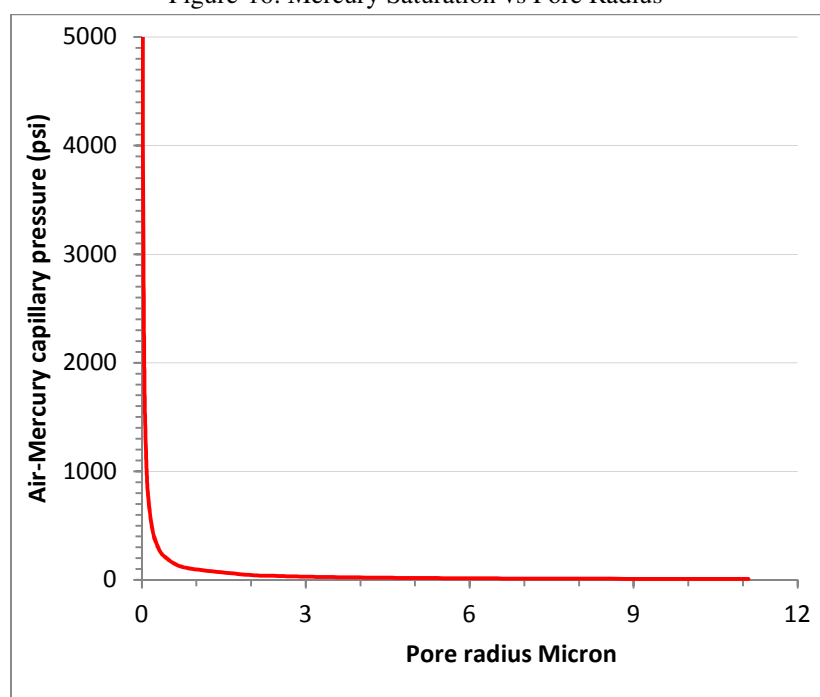


Figure-17: Air-Mercury Capillary Pressure vs Pore Radius

Conclusions

From this study about the Upper Cretaceous Dokan and Gulneri Formations at Khabbaz field in Kirkuk area of Northern Iraq. The following conclusions can be made:

1. Both formations (Dokan and Gulneri) have almost a regular thickness all over the field; the thickness of Dokan Formation ranged from 21 to 29 m, and Gulneri Formation from 11 to 14m.
2. Gulneri Formation is characterized by shale dominance, so it was excluded from further evaluation as reservoir unit. The majority of the interpretation focused on Dokan Formation, which is characterized by clean carbonate zone, with limestone dominance.

3. Porosity of the Dokan reservoir at Khabbaz field ranges between 3 and 14%. The secondary porosity makes a significant fraction of porosity which represents from 7% to 65% of the total porosities.
4. From Neutron –Density logs, the crossover of two curves is clearly observed along all well sections which indicate the gas saturation bearing reservoir.
5. The core plug porosity tests gave the average porosity of around 5.9%, and it is close to the primary porosity which is measured by sonic log, this type of porosity is mainly composed of matrix porosity and characterized by very low permeability. Hence, most of the porosity and the majority of the permeability came from the fractures.
6. The Capillary pressure is observed in mercury saturation for pore size of less than 2-micron, threshold pressure can be reached at mercury saturation of about 8-9 %.

Acknowledgments

Data and research materials for this study were provided by the Northern Oil Company (NOC), Kirkuk, to whom the author expresses his high gratitude.

References

- [1] AL-Qayim, B., Qadir, F., and AL-Biaty F. "Dolomitization and porosity evaluation of the Cretaceous Upper Qamchuqa (Mauddud) Formation, Khabbaz oil field, Kirkuk area, northern Iraq". *GeoArabia*, Vol 15, No. 4, pp. 49-76.(2010).
- [2] Asquith, G. B., and Gibson, C. R. "Basic Well Analysis for Geologist". AAPG, Tulsa, Oklahoma, USA.(1982).
- [3] Asquith, G., and Krygowski, D. "Basic Well Log Analysis". AAPG Method in Exploration Method, No.16. (2004).
- [4] Bateman, R. M. "Open-Hole Log Analysis and Formation Evaluation", 137 Newbury Street, Boston. (1985).
- [5] Bellen, R. C. Van., Dunnington, H. V., Wetzel, R., and Morton, D. "Lexique Stratigraphique International". ASIE, Fascicule 10 a, Iraq, Paris. (1959).
- [6] Buday, T. "The Regional Geology of Iraq, Vol. 1, Stratigraphy and Paleogeography". Dar Al-Kutub Publishing House, University of Mosul, Mosul, Iraq. (1980).
- [7] Buday, T., and Jasim, S. Z. "The Regional Geology of Iraq, Volume II; Tectonism, Magmatism and Metamorphism". Dar AL-Kutub Publishing House, University of Mosul. Iraq. (1987).
- [8] Dewhurst, D. N., Jones, R. M., and Raven, M. D. "Microstructural and Petrophysical Characterisation of Muderong Shale: Application to top seal risking". *Petroleum Geoscience*, Vol. 8, pp. 371-383, 1 December (2002).
- [9] Ghorab, M., Ramadan, A. M., and Nouh, A. Z. "The relation between shale origin (source or nonsource) and its type for Abu Roash Formation at Wadi-El Natrun area, south of Western Desert, Egypt," *Australian Journal of Basic Applied Sciences*, Vol. 2, No. 3, pp. 360-371. (2008).
- [10] Iraq Development Potential, "Oil and gas field infrastructure". (2003).
- [11] Jassim, S. Z. and Buday, T. "Units of the Unstable Shelf and the Zagros Suture", Chapter 6, in: Jassim, S. Z., and J.C. Goff, eds., "Geology of Iraq", first edition: Brno, Czech Republic, Prague and Moravian Museum, pp. 71-83. (2006).
- [12] Katz, A. J., and Thompson, A. H. "A quantitative prediction of permeability in porous rock Phys". *Rev. B* Vol. 34, pp. 8179–8181. (1986).
- [13] Katz, A. J., and Thompson, A. H. "Prediction of rock electrical conductivity from mercury injection measurements". *J. Geophys. Res.* Vol. 92, pp. 599–607. (1987).
- [14] North, F. K. "Petroleum Geology". Allen & Unwin Inc. (1985).
- [15] Qader, F., and Al-Qayim B. "Petrophysical and Sedimentological Characterization of the Aptian

- Shu'aiba (Lower Qamchuqa) Formation Reservoir at the Khabbaz Oilfield, Northern Iraq". *Journal of Petroleum Geology*, Vol. 39, No. 4, pp 375-392. (2016).
- [16] Qader, F., "Formation Evaluation of Upper Qamchuqa Reservoir, Khabbaz Oil Field, Kirkuk Area, Northeastern Iraq". Unpublished PhD thesis, University of Sulaimany.(2008).
- [17] Reeckman, A., and Friedman G. M. "Exploration for Carbonate Petroleum Reservoirs". Elf Aquitaine, John Wiley & Sons Inc., (1982).
- [18] Rider, M. "The Geological Interpretation of Well Logs". Second edition, Whittles Publishing, (2000).
- [19] Rider, M., and Kennedy, M. "The Geological Interpretation of Well Logs", Third Edition, Rider French Consulting Ltd., Aberdeen and Sutherland. (2011).
- [20] Selley, R. C. "Elements of Petroleum Geology", Second Edition, Academic Press, (1998).
- [21] Schlumberger, "The Essentials of Log Interpretation". (1982).
- [22] Schlumberger. "Log interpretation chart", Schlumberger Educational Services, U.S.A. (1988).

